Shukla for measuring the single-photon fluorescence lifetimes.

Registry No. 1, 134906-85-7; 2, 2928-43-0; 3, 90-43-7; 4, 134906-89-1; 5, 134906-86-8; 6, 134906-87-9; 7, 229-95-8; 8, 2005-10-9; 11, 29574-51-4; 12, 134906-90-4; 13, 883-20-5; 14, 52978-94-6; 18, 134906-91-5; 19, 134906-88-0; *cis*-20, 134906-92-6.

Supplementary Material Available: Tables of positional parameters, anisotropic thermal parameters, bond lengths, and angles (15 pages); tables of observed and calculated structure factors (11 pages). Ordering information is given on any current masthead page.

Crystal Structures of Self-Aggregates of Insoluble Aliphatic Amphiphilic Molecules at the Air–Water Interface. An X-ray Synchrotron Study

D. Jacquemain,[†] F. Leveiller,[†] S. P. Weinbach,[†] M. Lahav,[†] L. Leiserowitz,*[,†] K. Kjaer,[‡] and J. Als-Nielsen*[,‡]

Contribution from the Structural Chemistry Department, Weizmann Institute of Science, Rehovot 76100, Israel, and Physics Department, Risø National Laboratory, DK4000 Roskilde, Denmark. *Received February 14, 1991*

Abstract: Uncompressed insoluble amphiphilic molecules possessing linear hydrocarbon chains $C_nH_{2n+1}X$ (n = 23, 30, 31, X = OH; n = 29, X = COOH; and n = 19, X = $CONH_2$) spontaneously form large two-dimensional (2-D) crystalline clusters over pure water at low temperature (5 °C). These 2-D crystallites were detected and their structures were solved using grazing incidence X-ray diffraction (GID). Their packing arrangements are described in terms of 2-D space-group symmetry and hydrocarbon-chain packing. All the crystal structures display rectangular unit cells containing two molecules that are probably related by glide symmetry in the 2-D space group *pg* for the alcohol (X = OH) and the acid (X = COOH) and by translation symmetry in the 2-D space group *p*1 for the amide (X = $CONH_2$). The alcohol molecules are tilted by 8–11° from the vertical toward next-nearest neighbors, the tilt angle being dependent on the chain length. The amide and the acid molecules are tilted toward nearest neighbors by 18° and 26°, respectively. The positional correlation lengths of the crystallites were found to be anisotropic; they extend over only 35–95 spacings parallel to the molecular tilt direction, but over 135–270 spacings perpendicular to it. The similarity of chain packing in the 2-D crystallites and in three-dimensional (3-D) crystals of aliphatic amphiphilic molecules is clearly established. These crystallites may therefore, on the water surface, mimic crystallization mechanisms observed in 3-D systems.

Introduction

Evidence for the formation of self-organized two-dimensional (2-D) crystals composed of amphiphilic molecules at the air–water interface has, until recently, been indirect. For example, surface tension and oriented crystallization studies of *soluble* hydrophobic α-amino acids have brought forth evidence that they not only accumulate spontaneously but also form two-dimensional crystalline aggregates (crystallites) at the solution surfaces.[1-3] Studies of oriented crystallization extended to *insoluble* amphiphilic α-amino acid molecules forming Langmuir monolayers also brought evidence for the spontaneous formation of crystallites at the solution surface, even when the amphiphilic molecular concentration at the surface is very low.[3b] Epifluorescence measurements gave a visual confirmation of the spontaneous aggregation of insoluble amphiphilic molecules at the water surface and furnished some information on the orientational order and on the morphology of the aggregates on the micron level.[4] However, these studies provide no direct information on the crystallite size and structure on the molecular level. The newly developed synchrotron X-ray surface technique of grazing incidence X-ray diffraction[5] (GID) is a powerful tool for exploring this field since it allows for the detection of crystallites formed by insoluble amphiphilic molecules and for the determination of their size and structure almost at the atomic level. We were not able to detect crystalline self-aggregation of uncompressed monolayers of α-amino acid surfactants with hydrocarbon chains at room temperature.[5b] However, we did observe the spontaneous formation of crystallites of the α-amino acid amphiphile $CF_3(CF_2)_9(CH_2)_2OCOCH_2CH(NH_3^+)CO_2^-$ at room temperature[6] with a lateral ordering range exceeding 1500 Å. More recently, crystalline self-aggregation has been observed by GID for the fluorinated acid[7] $C_{10}F_{21}CH_2COOH$. It was concluded for both systems that nearly all the molecules are in the crystalline phase.

Here, we report GID results from insoluble aliphatic amphiphilic molecules in the uncompressed state at the air–water interface. Monolayers with hydrocarbon chains proved to be less crystalline than those with fluorocarbon chains in their uncom-

[†] Weizmann Institute of Science.
[‡] Risø National Laboratory.

(1) Weissbuch, I.; Addadi, L.; Berkovitch-Yellin, Z.; Gati, E.; Lahav, M.; Leiserowitz, L. *Nature* **1984**, *310*, 161.
(2) Weissbuch, I.; Frolow, F.; Addadi, L.; Lahav, M.; Leiserowitz, L. *J. Am. Chem. Soc.* **1990**, *112*, 7718.
(3) (a) Landau, E. M.; Levanon, M.; Leiserowitz, L.; Lahav, M.; Sagiv, J. *Nature* **1985**, *318*, 353. (b) Landau, E. M.; Grayer Wolf, S.; Levanon, M.; Leiserowitz, L.; Lahav, M.; Sagiv, J. *J. Am. Chem. Soc.* **1989**, *111*, 1436.
(4) (a) Von Tscharner, V.; McConnell, H. M. *Biophys. J.* **1981**, *36*, 409. (b) Lösche, M.; Möhwald, H. *Rev. Sci. Instrum.* **1984**, *55*, 1968. (c) Moore, G. B.; Knobler, C. M.; Akamatsu, S.; Rondelez, F. *J. Phys. Chem.* **1990**, *94*, 4588.
(5) (a) Kjaer, K.; Als-Nielsen, J.; Helm, C. A.; Laxhuber, L. A.; Möhwald, H. *Phys. Rev. Lett.* **1987**, *58*, 2224. (b) Grayer Wolf, S.; Leiserowitz, L.; Lahav, M.; Deutsch, M.; Kjaer, K.; Als-Nielsen, J. *Nature* **1987**, *328*, 63. (c) Barton, S. W.; Thomas, B. N.; Flom, E. B.; Rice, S. A.; Lin, B.; Peng, J. B.; Ketterson, J. B.; Dutta, P. *J. Chem. Phys.* **1988**, *89*, 2257. (d) Helm, C. A.; Möhwald, H.; Kjaer, K.; Als-Nielsen, J. *Biophys. J.* **1987**, *52*, 381. (e) Kjaer, K.; Als-Nielsen, J.; Helm, C. A.; Tippman-Krayer, P.; Möhwald, H. *J. Phys. Chem.* **1989**, *93*, 3200.
(6) Jacquemain, D.; Grayer Wolf, S.; Leveiller, F.; Leiserowitz, L.; Lahav, M.; Deutsch, M.; Kjaer, K.; Als-Nielsen, J. *J. Am. Chem. Soc.* **1990**, *112*, 7724.
(7) Barton, S. W.; Coudort, Rondelez, F.; Lin, B.; Novak, Rice, S. A. Manuscript in preparation.

0002-7863/91/1513-7684$02.50/0

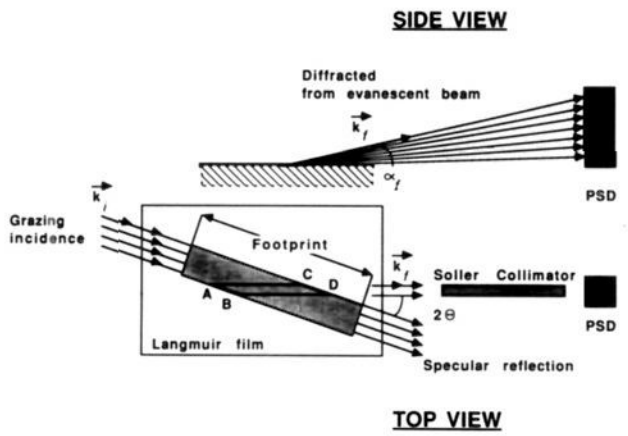

Figure 1. Top and side views of the GID geometry. The footprint of the grazing incidence beam is indicated by the darker area. The position-sensitive detector (PSD) has its axis along the vertical direction z. Only the area ABCD contributes to the measured scattering. $\mathbf{k}_i$ and $\mathbf{k}_f$ are the incident and outgoing wave vectors. The scattering vector $\mathbf{q}$ is given by $\mathbf{k}_f - \mathbf{k}_i$.

pressed state at room temperature. Indeed, no crystalline order could be detected under such conditions for aliphatic monolayers of an α-amino acid,[5b] an alcohol,[5c] and a phospholipid.[5d] Monolayers of arachidic acid[5e] exhibited lateral crystalline ordering of the order of several 100 Å in coexistence with a fluid phase. This may be related to the observation that hydrocarbon chains are less stiff than fluorocarbon chains[6,8] and so more prone to conformational disorder. A pronounced decrease of such disorder upon reduction of temperature has been indicated by GID studies of fatty acid and alcohol monolayers over water.[9] Thus, we studied by GID at low temperature (5 °C) three classes of insoluble amphiphiles of general formula $C_nH_{2n+1}X$: primary alcohol (X = OH), carboxylic acid (X = COOH), and primary amide ($X = CONH_2$). The results indicate crystalline self-aggregation of all of these molecules and reveal different crystallite structures, depending on the nature of the hydrophilic moiety.

Experimental Section

Materials. Triacontanoic acid (n = 29, X = COOH) and 1-triacontanol (n = 30, X = OH) were purchased from Sigma (purity 99%) and used without further treatment. The alcohols tricosanol (n = 23, X = OH) and hentriacontanol (n = 31, X = OH) were obtained by reduction of the corresponding methyl esters (Sigma, purity 99%). Arachidic acid (Sigma, purity 99%) was converted into arachidamide (n = 19, $X = CONH_2$) in two steps: the formation of the chloride derivative by action of $SOCl_2$ followed by treatment with ammonia. Purities were checked by thin-layer chromatography, and the identity of the compounds was checked by NMR and IR. Spreading solutions of the amphiphiles were prepared in chloroform (Merck, analytical grade) with concentrations close to 5×10^{-4} M. The monolayers were spread at approximately room temperature over Millipore water before cooling the subphase.

Experimental Set-Up. The measurements on monolayers were carried out using the liquid-surface diffractometer on beam line D4 at Hasylab, DESY, Hamburg. A sealed and thermostated Langmuir trough equipped with a Wilhelmy balance was mounted on the diffractometer. The temperature in the trough was measured by a probe under the water surface, and the thermostat was set to 5 ± 1 °C. The synchrotron radiation beam was monochromated to a wavelength λ = 1.39 Å by Bragg reflection from a Ge(111) crystal and was adjusted to strike the surface at an incident angle $\alpha = 0.85\alpha_c$, where $\alpha_c = 0.138°$ is the critical angle for total external reflection, to maximize surface sensitivity.[10,11] The dimensions of the footprint (Figure 1) of the incoming X-ray beam on the liquid surface were 50 × 5 mm.

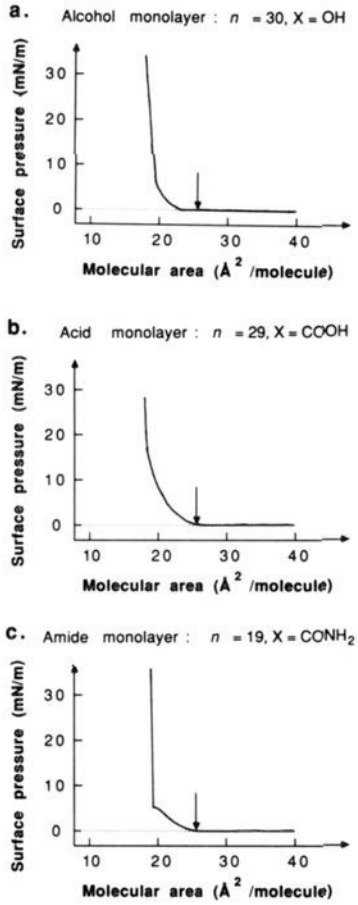

Figure 2. Surface pressure–area diagrams at 5 °C over Millipore water. The arrow indicates the monolayer state for which the GID data presented here were taken: (a) 1-triacontanol monolayer; (b) triacontanoic acid monolayer; (c) arachidamide monolayer.

The diffraction condition for 2-D crystals lying in the xy plane is that the component of the scattering vector in the horizontal plane, labeled $\mathbf{q}_{xy}$ ($q_{xy} \approx 4\pi \sin\theta/\lambda$, where 2θ is the horizontal angle between the incident and the diffracted beam, as shown in Figure 1), must coincide with a reciprocal lattice vector $\mathbf{G}_{hk}$ ($\mathbf{G}_{hk} = 2\pi(h\mathbf{a}^* + k\mathbf{b}^*)$ where $\mathbf{a}^*$ and $\mathbf{b}^*$ are the reciprocal lattice vectors and h and k are the integer components of the corresponding lattice point (the bold-face letters indicate vectors)). There is no selection rule or restriction on the component of the scattering vector along the normal to the film, defined as $\mathbf{q}_z$ ($q_z = 2\pi \sin\alpha_f/\lambda$, where α_f is the angle between the diffracted beam and the water surface, shown in Figure 1). Therefore, the GID patterns from Langmuir monolayers arise from a 2-D array of rods,[10-13] labeled Bragg rods (BR), which extend parallel to $\mathbf{q}_z$.

The monolayers are composed of crystallites azimuthally randomly oriented on the water surface and so may be described as 2-D "powders".[5] Thus, the collection of the diffracted radiation was made in two ways using a position-sensitive detector (PSD, Figure 1), which intercepted photons over a range $0.0 \le q_z \le 0.9$ Å^{-1}. The scattered intensity measured by scanning different values of q_{xy} and integrating over the whole q_z-window of the PSD yields *Bragg peaks*. Simultaneously, the scattered intensity recorded in channels along the PSD, but integrated over q_{xy} produces q_z-resolved scans called *Bragg rod profiles*.

Several different types of information were extracted from the measured profiles. A measure of the range of crystalline order can be obtained by shape analysis[14] of the Bragg peaks, also, the 2-D crystal lattice

(8) (a) Dixon, D. A.; van Catledge, F. A.; Smart, B. E. *Abstracts of the 9th International Union of Pure and Applied Chemistry Conference on Physical and Organic Chemistry*; 1988; p A15. (b) Potential energy calculation performed on model structures of fluorocarbon and hydrocarbon chains have indicated that the packing energy is distinctly lower for the former.

(9) (a) Bohanon, T. M.; Lin, B.; Shih, M. C.; Ice, G. E.; Dutta, P. *Phys. Rev. Lett.* **1990**, *65*, 191. (b) Lin, B.; Peng, J. B.; Ketterson, J. B.; Dutta, P.; Thomas, B.; Buotempo, J.; Rice, S. A. *J. Chem. Phys.* **1989**, *90*, 2393. (c) Kenn, R. M.; Böhm, C.; Bibo, A. M.; Peterson, I. R.; Möhwald, H.; Kjaer, K.; Als-Nielsen, J. *J. Phys. Chem.* **1991**, *95*, 2092.

(10) Als-Nielsen, J.; Kjaer, K. *The Proceedings of the Nato Advanced Study Institute, Phase Transitions in Soft Condensed Matter*; Geilo, Norway, April 4–14, 1989; Riste, T., Sherrington, D., Eds.; Plenum Press: 1989; pp 113–137.

(11) Feidenhans'l, R. *Surf. Sci. Rep.* **1989**, *10*(3), 105.

(12) Jacquemain, D.; Grayer Wolf, S.; Leveiller, F.; Lahav, M.; Leiserowitz, L.; Deutsch, M.; Kjaer, K.; Als-Nielsen, J. *Colloque de Physique* **1989**, *50*, suppl. no. 10, colloque C7, 29.

(13) Vineyard, G. *Phys. Rev. Lett.* **1982**, *B26*, 4146.

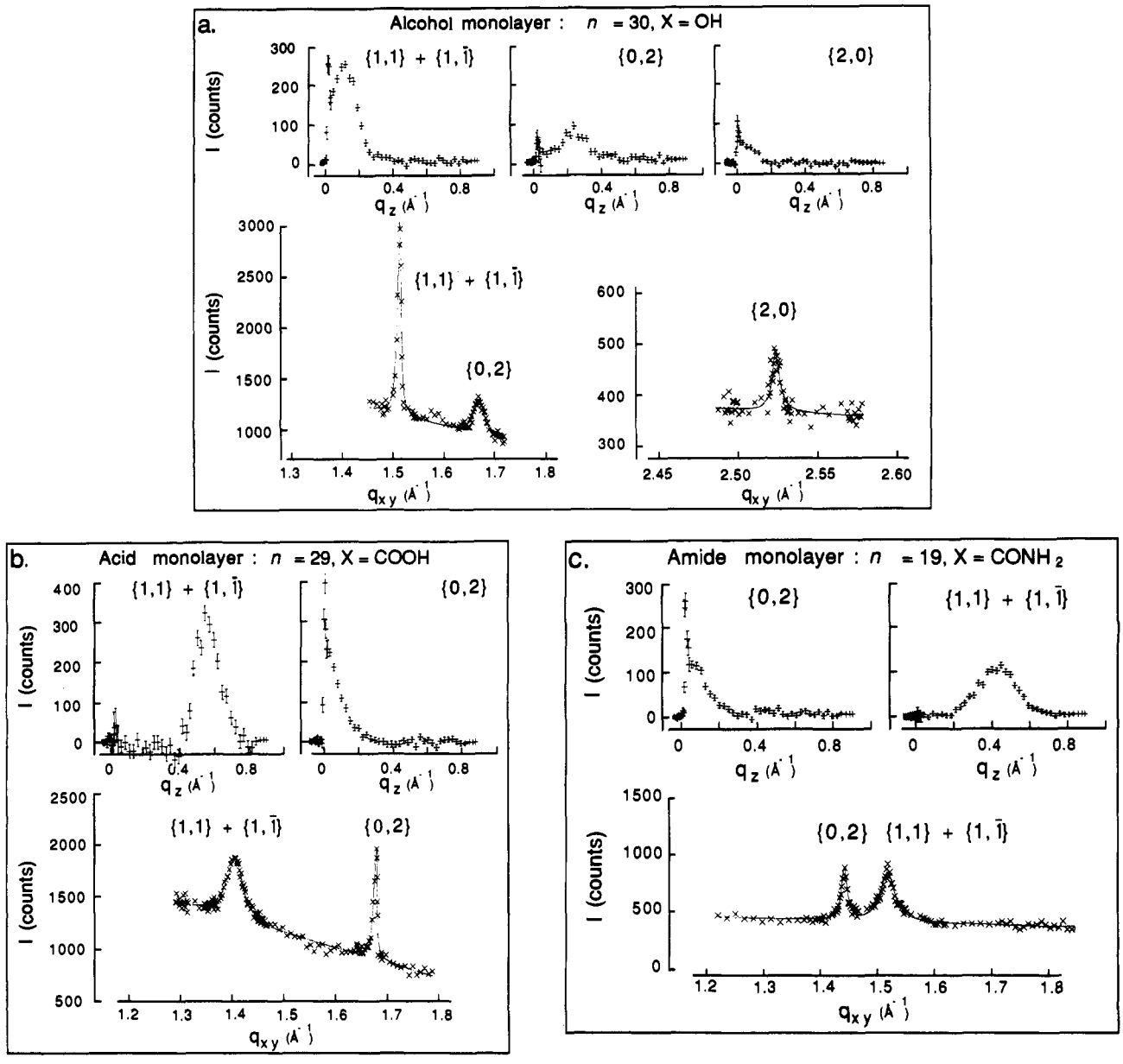

Figure 3. Grazing incidence X-ray diffraction spectra of monolayers at zero surface pressure and at 5 °C over pure water. Top. q_z-resolved Bragg rod profiles. The sharp peak observed around 0.01 Å^{-1} is due to the interference of rays diffracted upward with rays diffracted down and subsequently reflected back up by the interface.[13] Bottom. q_z-integrated Bragg peaks. The $\{h,k\}$ reflection assignment is indicated on the two data sets: (a) 1-Triacontanol monolayer. Note the change in q_{xy} and intensity scale for the {2,0} reflection. (b) Triacontanoic acid monolayer. (c) Arachidamide monolayer.

parameters (a, b, γ) can be extracted, using the Bragg formula, from the position of the maxima of the Bragg peaks. The intensity profiles of the Bragg rods are modulated by the molecular X-ray structure factor of the diffracting amphiphilic molecules and give precise information on the molecular orientation in the 2-D crystal.[10,12] Assuming that the aliphatic tails are uniformly and rigidly tilted in the monolayer, the angle t between the molecular axis and the surface normal is given by[10,12]

$$\cos \psi_{hk} \tan t = q_z^{\circ}/|\mathbf{G}_{hk}|$$

where q_z° is the position of the maximum along the Bragg rod and ψ_{hk} is the azimuthal angle between the tilt direction projected on the xy plane and the reciprocal lattice vector $\mathbf{G}_{hk}$. The molecules will therefore be perpendicular to the surface when, for all reflections (h,k), q_z° tends to 0 Å^{-1}. Denoting the molecular areas by A_0 and A_t for the untilted and tilted states, respectively, the tilt angle t can also be determined by $\cos t = A_0/A_t$, assuming close packing of the hydrocarbon chains in both states.[10]

Results

The pressure–area diagrams over Millipore water for the acid, one alcohol (n = 30), and the amide are displayed in Figure 2a–c, respectively. These show for each compound the point where the GID data were collected at 5 ± 1 °C (at zero surface pressure and for an average molecular area of 25 Å^2). The diffraction patterns for the same compounds follow in Figure 3. All the compounds give rise to two low-order reflections. For the interpretation of the diffraction data we refer to known three-dimensional (3-D) crystal structures of molecules with long hydrocarbon chains. These structures are composed of layers in which the molecules are surrounded by six nearest neighbors, giving rise to 2-D lattices that can be described for the case of one molecule per unit cell as hexagonal, distorted hexagonal, or oblique,[15,16] depending upon the 2-D space-group symmetry. A

(14) (a) The PSD is mounted vertically behind a horizontally collimating Soller slit (Figure 1) of resolution $\Delta(q_{xy}) = 0.007$ Å^{-1} (full width at half-maximum (FWHM)). For a measured diffraction peak of width FWHM-(q_{xy}), the Debye–Scherrer formula allows one to compute the coherence length L: $L = 0.90[2\pi/[\mathrm{FWHM}(q_{xy})^2 - \Delta^2]^{1/2}]$, where Δ is the soller collimator's resolution limit. (b) Guinier, A. *X-ray Diffraction*; Freeman: San Francisco, 1968; pp 121–125.

(15) Abrahamsson, S.; Dahlen, B.; Löfgren, H.; Pascher, I. *Progress in the Chemistry of Fats and Other Lipids*; Pergamon Press: New York, 1978; Vol *16*, 125.

Table I. Results of Bragg Peak Analysis for the Different Monolayers $C_nH_{2n+1}X$[a]

compd *n*, X	d_{11} and $d_{1\bar{1}}$ (*L*)	d_{02} (*L*)	d_{20} (*L*)	*a* (a_s)	*b* (b_s)	$A_t = ab/2$	A_0	t_{BR}	t_{area}
23, OH	4.18	3.78	2.50	5.00	7.56	18.90	18.45	9.5	12.5
	(≥1000)	(360)	(≥1000)	(5.00)	(7.46)				
30, OH	4.15	3.75	2.49	4.99	7.49	18.69	18.45	7.7	9.2
	(≥1000)	(230)	(≥1000)	(4.99)	(7.42)				
31, OH	4.16	3.77	2.49	4.99	7.53	18.79	18.45	10.1	10.9
	(≥1000)	(270)	(700)	(4.99)	(7.41)				
29, COOH	4.44	3.72		5.53	7.44	20.57	18.55	26.8	25.6
	(150)	(≥1000)		(4.94)	(7.44)				
19, $CONH_2$	4.34	4.12		4.69	8.69	20.38	19.17	19.0	19.8
	(200)	(550)							

[a] The *d*-spacings (in Å) for each {*h*,*k*} reflection are given together with the positional correlation length *L* (in Å) associated with the reflection. The unit cell parameters *a*,*b* (in Å) are calculated for a centered rectangular cell. a_s and b_s are the calculated lengths of the orthorhombic projected cell for the acid and the alcohols monolayers (see text for details): $a_s = a \cos t$, $b_s = b$ if the molecular tilt is along the *a* axis, $a_s = a$, $b_s = b \cos t$ if the molecular tilt is along the *b* axis, where the tilt angle *t* is determined from the Bragg rod data. A_0 and A_t, the areas (in Å^2) in the vertical compressed and tilted uncompressed phase, are both calculated from GID data. t_{BR} and t_{area} are the molecular tilts (in degrees) in the tilted uncompressed phase as determined, respectively, from Bragg rod data and the A_0/A_t ratio (see Experimental Section). Note that the tilt determination using Bragg rod intensity profiles is more accurate than when using a comparison of areas. The experimental standard deviation for t_{BR} values can be estimated to be 1° but it is of the order of a few degrees for t_{area} values.

crystalline monolayer over water composed of a 2-D "powder", appearing in an oblique cell, would give rise to three (resolved) low-order GID reflections, a centered rectangular (or distorted hexagonal) cell to two such reflections,[17] and a hexagonal cell to one. The GID results point to a rectangular cell for which the symmetry related {1,1} and {1,$\bar{1}$} reflections coincide and the {0,2} reflection is distinct.[18] This deduction is further supported by the observation for the alcohols of a higher order reflection that could be indexed {2,0} in the centered rectangular cell. Hence, the unit-cell parameters were computed for a centered rectangular cell and are listed in Table I for each compound. The crystallite correlation lengths[19] (*L*) associated with the first-order reflections show that the range of crystalline order is anisotropic. For the sharpest reflections observed, *L* extends to at least 1000 Å for the alcohols and the acid and to 550 Å for the amide (Table I). We have also obtained diffraction data for the same monolayers in the compressed state at surface pressures of about 20 mN/m (not shown here). The Bragg rod data indicate that the compressed molecules stand vertically on the water surface. The corresponding molecular areas A_0 are listed in Table I.

Alcohol Monolayers (X = OH). The diffraction patterns for the three alcohols (*n* = 23, 30, and 31) were similar except for small differences in peak position (Table I). The Bragg rod intensity profile for the high-order {2,0} reflection has its maximum at $q_z^\circ = 0$ Å^{-1} (Figure 3a). Hence, the molecular axis lies in a plane perpendicular to the short *a* axis of the unit cell and so the hydrocarbon chains can only be tilted toward next-nearest neighbors in the direction of the long *b* axis (Figure 4a). This deduction is compatible with the intensity profiles observed for the {1,1} + {1,$\bar{1}$} reflections and the {0,2} reflection. From the q_z° values measured on these Bragg rod profiles, tilt angles of 10°, 8°, and 11° from the surface normal were obtained for *n* = 23, 30, and 31, respectively.[20]

As mentioned previously, the chain tilt angle *t* can be estimated from the ratio $A_0/A_t = \cos t$, where A_0 and A_t correspond to the crystal unit cell areas in the compressed and uncompressed states, respectively. The values of A_0 (Table I) were derived from the GID measurements of the compressed monolayers.[21a] The tilt angles are 13°, 9°, and 11° for *n* = 23, 30, and 31, respectively, in good agreement with the determination from the Bragg rod maxima positions.[21b]

Acid (X = COOH) and Amide (X = $CONH_2$) Monolayers. The intensity profile of the Bragg rods for the low-order {0,2} reflection has its maximum[22] at $q_z^\circ = 0$ Å^{-1} (Figure 3b,c). Hence, the molecular axis in these systems lies in a plane perpendicular to the long *b* axis of the unit cell. Therefore, the hydrocarbon chains are tilted toward the nearest neighbors along the short *a* axis of the rectangle (Figure 4b,c). This deduction is compatible with the intensity profile observed for the {1,1} + {1,$\bar{1}$} reflections. From the q_z° values measured on the Bragg rod profile, tilt angles of 26° and 18° from the surface normal were obtained for the acid and the amide, respectively.[20]

In the compressed state, the acid and amide molecules stand vertically on the surface and occupy molecular areas A_0 = 18.57 and 19.17 Å^2 (Table I), compared with their molecular areas in the uncompressed state A_t = 20.58 and 20.35 Å^2, respectively (Table I). These values yield molecular tilt angles of 26° and 20°, in good agreement with the values derived from the Bragg rod profiles.

Discussion

The diffraction results indicate the existence at zero pressure of spontaneously formed crystallites of amphiphilic aliphatic molecules possessing different hydrophilic moieties. Moreover, the Bragg rod data can be used for a precise determination of the packing arrangement of molecules in the crystallites. We have only used the positions of the Bragg rod maxima q_z° to derive the magnitude and the lateral direction of the molecular tilt. We have not yet discussed the orientation of the plane of the carbon chain around the molecular axis. In order to establish a plausible model we shall take advantage of the known 3-D crystal structures of molecules with long hydrocarbon chains as we did in previous studies.[5b,6,23] This strategy is meaningful because these 3-D structures can be described as a stack of layers of molecules; thus, the molecular arrangement in a single layer therein may well resemble that of the monolayer.

(16) Small, D. M. The Physical Chemistry of Lipids. In *Handbook of Lipid Research*; Plenum Press, New York, 1986; Vol. *4*, Chapters 2, 5 and 8.

(17) A centered rectangular lattice results from a small uniaxial distortion along a symmetry direction of the hexagonal lattice. Distortion along a nonsymmetry direction leads to an oblique lattice.

(18) The notation {*h*,*k*} refers to both (*h*,*k*) and ($\bar{h}$,$\bar{k}$) coinciding reflections.

(19) The correlation length *L* associated with the GID {*h*,*k*} reflection corresponds to the average length of all diffracting crystallites over which "perfect" crystallinity extends in the direction of the reciprocal lattice vector G_{hk}.

(20) In a centered rectangular cell, if the chain tilt direction is along the axis *a*, $\cos \psi_{11} = \cos \psi_{1\bar{1}} = [1 + (a/b)^2]^{-1/2}$ and $\cos \psi_{02} = 0$; if the tilt direction is along *b*, $\cos \psi_{11} = \cos \psi_{1\bar{1}} = [1 + (b/a)^2]^{-1/2}$ and $\cos \psi_{02} = 1$.

(21) (a) The GID results for the compressed monolayers of these compounds will be published at a later date. (b) The discrepancy of 3° in the tilt determination by the two methods for the shortest chain alcohol (*n* = 23) may be due to a chain-length effect. The melting point of 3-D crystals of long-chain fatty alcohols[21c] decreases with decreasing chain length, suggesting that the thermal motion is higher for the shortest alcohols. This might explain why the shortest alcohol studied here has the largest molecular area in the uncompressed state (Table I). (c) Watanabe, A. *Bull. Chem. Soc. Jpn.* **1961**, *34*, 1728; Ibid. **1963**, *36*, 336.

(22) For the amide monolayer the {0,2} reflection actually peaks at a q_z° value close to 0.04 Å^{-1}, implying that the molecular axis lies slightly off the plane perpendicular to the *b* axis (by an angle of about 3°).

(23) Grayer Wolf, S.; Deutsch, M.; Landau, E. M.; Lahav, M.; Leiserowitz, L.; Kjaer, K.; Als-Nielsen, J. *Science* **1988**, *242*, 1286.

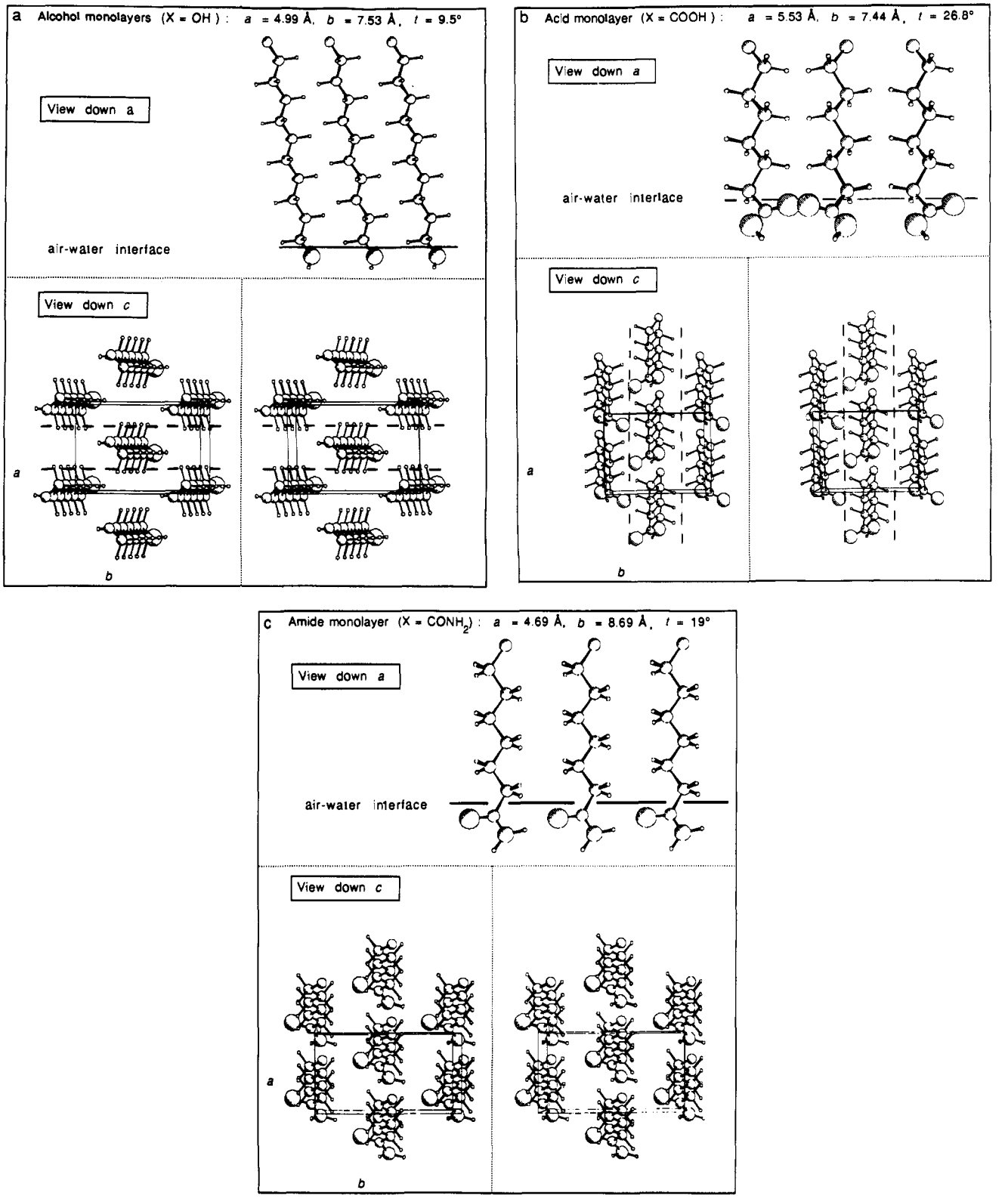

Figure 4. Stereospecific view of the packing arrangement, seen perpendicular to the water surface, and a side view along a direction parallel to the water surface of models of the hydrocarbon-chain packing in the crystallites formed at 5 °C over pure water. For clarity only the head group and maximally 11 CH_2 groups of each molecule are shown. On the last carbon atom drawn the hydrogen atoms are omitted. The glide symmetry elements, when present, are shown as dashed lines in the conventional way.[33b] Note that for convenience the origin of the unit cell is placed halfway between adjacent glide planes. The rectangular cell (a,b) is indicated: (a) alcohol monolayers (space group pg); (b) triacontanoic acid monolayer (space group pg); (c) arachidamide monolayer (space group $p1$).

Hydrocarbon Chains Packing in the Crystallites: Orthogonal Packing versus Parallel Packing.[24] We shall now consider the principal ways of packing long aliphatic chains, whose molecular axes are parallel, into layers, neglecting head-group effects. Close packing between neighboring hydrocarbon chains can occur if the hydrogen atoms of adjacent molecules intermesh. This condition for close molecular packing implies (primarily) two distinct packing motifs.[25] In one type, all of the chains are related by

(24) In the Discussion, the notation (a', b', c') and (a'_s, b'_s, c'_s) are used to describe the unit cell and the subcell axes of the 3-D crystal structures and (a, b) and (a_s, b_s) for the unit cell and the projected cell axes of the monolayers.

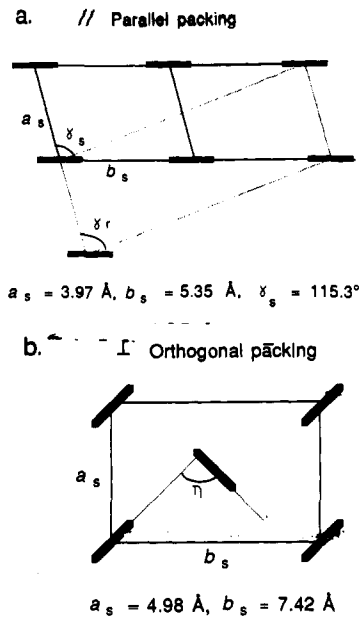

Figure 5. Schematic representation of the hydrocarbon chain packing. The black sticks symbolize the projection of the carbon chains onto a plane perpendicular to the molecular axis. (a) Parallel packing in a 2-D oblique subcell (the subcell represented here corresponds to the triclinic parallel packing $T_\parallel$). The centered cell closest to rectangular geometry is drawn in dotted lines to show the deviation from rectangular geometry. The angle γ_r provides a measure of this deviation. (b) Orthogonal $O_\perp$ packing in the 2-D orthorhombic subcell. η is the dihedral angle between the planes containing the carbon chains of neighboring molecules.

simple translation (Figure 5a) and are thus mutually parallel ($\parallel$), forming arrangements that can be described as triclinic $T_\parallel$ or monoclinic parallel[26] $M_\parallel$. In the other motif the chains are related by a glide so that neighboring chains are approximately in a mutually perpendicular orientation ($\perp$); the motif (Figure 5b) is described as orthorhombic orthogonal $O_\perp$. The long-chain alcohols (X = OH) and acids (X = COOH) possess crystal structures that belong to this classification.[16,25] There are exceptions to these packing types, in particular for compounds in which hydrogen bonds at the head groups play a dominant role in deciding the structure, as in the case for long-chain amide molecules.[27]

Thus, we first discuss 3-D crystal structures of the alcohols and acids. The most stable layer structures were shown to be of the orthorhombic orthogonal $O_\perp$ type[16,25]. In a layer with such packing, the hydrocarbon chains are related by glide symmetry and the resulting dihedral angle η between the molecular planes through their carbon atoms is approximately 90° (Figure 5b). Common to all these structures are the parameters of the orthorhombic $O_\perp$ subcell[16,25] (Figure 5b), which is a projection of the unit cell onto a plane perpendicular to the molecular axis. The subcell may be regarded as rectangular with dimensions a'_s = 4.98 Å, b'_s = 7.42 Å, corresponding to a cross-sectional area A_s = 18.48 Å^2. Some 3-D crystal structures of alcohols and acids possessing long hydrocarbon chains appear in the triclinic $T_\parallel$ packing motif,[16,25] yielding a 2-D oblique subcell a'_s = 3.97 Å, b'_s = 5.35 Å, γ'_s = 115.3° in the crystal layers[26,28] (Figure 5a). The oblique character of this subcell can be measured in terms of the centered subcell shown in Figure 5a, where the deviation from the rectangular geometry given by the angle γ_r is equal to 86.7°. The monoclinic $M_\parallel$ type of packing has not been observed in 3-D crystal structures of simple carboxylic acids and alcohols possessing long hydrocarbon chains.[27]

Combining these considerations with the GID results, we can establish the packing arrangements of the alcohol and acid monolayer crystals. The calculated 2-D cells (a_s,b_s) projected onto the monolayer plane (Table I) perfectly match the orthorhombic $O_\perp$ subcell of long-chain alcohol and acid 3-D crystal structures.[29] We may preclude a monolayer packing arrangement akin to the triclinic $T_\parallel$ structure, for that would yield the 2-D oblique projected cell (Figure 5a) completely different than the observed projected cell (Table I and Figure 5b), and three resolvable in-plane diffraction peaks would be observed. Thus, all of the data indicate that the alcohol and acid monolayer molecules appear in the orthorhombic $O_\perp$ packing motif (Figure 5b).

In 3-D crystals belonging to the orthorhombic $O_\perp$ class, the molecular chain axis is parallel to the glide plane to ensure the "herring-bone" motif (Figure 5b), but more to the point, to ensure that intermolecular contacts between methylene CH_2 groups of the glide-related molecules will be the same along the chain. Furthermore, parallel-chain axes preclude interpenetration between glide-related rows of closely packed molecules. Since the glide may be either parallel to the short a' or the long b' axis, there are two distinct ways in which the molecules tilt, either in the direction of a' or b'.[16] When the molecular axis tilts in the direction of the short a'_s axis of the subcell, the structure is of the β type.[16] When the tilt is in the direction of the long b'_s axis, the modification is labelled γ.[16] In order to preserve the local relationships between neighboring zig-zag chains, the tilt occurs only stepwise, carbon by carbon, and so the modifications are subclassified γ_i or β_i, where i is an integer index specifying the discrete tilt value.[16,30] In the orthorhombic subcell, the van der Waals interactions between the chains are optimal,[16,25] thus, the molecules can be considered as being in "close contact". As a result, the true (a',b') cell dimensions in the layer of the 3-D crystal for a given tilt angle t can be directly obtained from the subcell's dimensions (a'_s,b'_s): for the β_i form $a' = a'_s/\cos t_i$, $b' = b'_s$, and for the γ_i form, $a' = a'_s$, $b' = b'_s/\cos t_i$.

Structure of the Alcohol Crystallites. The Bragg rod profiles of the alcohol 2-D crystallites indicate, as for the γ form of the 3-D crystals, a molecular tilt of approximately 10° in the direction of the long axis b of the rectangular cell. However, no known γ form of an alcohol yields a chain packing directly comparable to the one observed in the 2-D alcohol crystallites; the lowest molecular tilt measured (corresponding to the γ_2 modification) is about 19° from the normal to the layer.[31] On the basis of all

(25) Kitaigorodski, A. I. *Organic Chemical Crystallography*; Consultants Bureau Press: New York, 1961; Chapter 4, p 117.

(26) These parallel packings can be described in terms of subcells[16,25] whose parameters are a'_s, b'_s, c'_s, α'_s, β'_s, γ'_s. For the $T_\parallel$ packing, the subcell is triclinic ($\alpha'_s \neq 90°$, $\beta'_s \neq 90°$, $\gamma'_s \neq 90°$), and for the $M_\parallel$ packing, the subcell is monoclinic ($\alpha'_s = \beta'_s = 90°$, $\gamma'_s \neq 90°$).

(27) (a) The 3-D crystal structures that were reported to exhibit a monoclinic $M_\parallel$ packing motif[27b-d] are systems where the molecules within the layer are directly interlinked by hydrogen bonds or where the chain packing is modified by the replacement of a methylene CH_2 group by sulfur atoms. In these packing arrangements, the molecular axis is tilted by 33–37° relative to the normal to the plane of the hydrophilic groups. We note that the monoclinic packing motif $M_\parallel$ yields, as in the triclinic packing motif $T_\parallel$, a 2-D oblique subcell in the layer. The subcell parameters differ widely depending upon the system, and there is no characteristic average subcell dimensions for this class of compounds. The diffraction pattern from a monolayer packing in an oblique cell should consist of three distinct diffraction peaks, and we observe only two. Note that a deviation of only 2° in the angle γ_r (Figure 5a) from the ideal value of 90° (rectangular geometry) is enough to produce three resolved diffraction signals. These arguments leave very little probability for a monoclinic type of packing. (b) Abrahamsson, S.; Westerdahl, A. *Acta Crystallogr.* **1963**, *16*, 404. (c) Larson, K. *Ark. Chemie* **1965**, *23*, 29. (d) Dahlen, B.; Lunden, B.-M.; Pascher, I. *Acta Crystallogr.* **1976**, *B32*, 2059.

(28) The triclinic $T_\parallel$ subcell of the crystal structure of *n*-octadecane is taken as a reference.[16] It is defined by a'_s = 4.29 Å, b'_s = 5.41 Å, c'_s = 2.54 Å, α'_s = 81.0, β'_s = 112.2°, γ'_s = 121.8°. We are mainly interested in the subcell projection onto a plane perpendicular to the molecular axis that is parallel to the subcell axis c'_s. This yields a 2-D oblique projected cell (given in the text and Figure 5a), which we derive as follows: $a_s = a'_s \sin \beta'_s$, $b_s = b'_s \sin \alpha'_s$, $\gamma_s = 180 - \gamma'_s{}^*$ (where $\gamma'_s{}^*$ is the angle in reciprocal space between the reciprocal lattice vectors $\mathbf{a}'_s{}^*$ and $\mathbf{b}'_s{}^*$).

(29) There are slight deviations from the ideal orthorhombic subcell dimensions (a'_s = 4.98 Å, b'_s = 7.42 Å). These variations in the subcell dimensions (Table I) may be due to the presence of the functional groups OH or COOH, as was found for 3-D crystal structures bearing a similar packing.[16]

(30) The possible tilt values for the β_i or γ_i modifications are imposed by close contact of the jth methylene group (CH_2) in one molecule with the ($j \pm i$)th group of the neighboring molecule.

of the data, we propose that the alcohol chains pack in a *primitive* rectangular cell[32] in which the molecules are related by glide symmetry (Figure 4a) compatible with what has been observed in 3-D crystals of the γ type. The glide is parallel to the b axis, the corresponding 2-D space group[33] is *pg*, and the chain packing is of the orthorhombic $O_\perp$ type. The low molecular tilt in the 2-D crystallites compared with tilt values observed in 3-D crystal structures may have been induced by a difference of interactions at the polar hydroxyl OH groups. Indeed, there are strong indications that the layer of hydroxyl groups organizes so as to satisfy hydrogen bonding with water molecules. Note that the alcohol unit cell parameters, in terms of a distorted hexagonal cell, are $a = b = 4.5$ Å, $|a + b| = 4.9$ Å, $\gamma = 113°$. If one assumes that the OH groups lie halfway between the adjacent glide planes in the primitive rectangular cell of the monolayer (i.e., at the four corners and at the center of the cell, see Figure 4a), the lattice of these OH groups has also a repeat unit given by the distorted hexagonal cell $a = b = 4.5$ Å, $\gamma = 113°$. Such an assumption seems reasonable since distances of the order of 4.5 Å are favorable for the hydrogen bonding of a water molecule to two neighboring hydroxyl groups. This deduction is in keeping with the observation than in the (001) face of hexagonal ice at 0 °C for instance, the hydrogen-bonded water molecules are arranged in the hexagonal cell[34] $a = b = 4.5$ Å, $\gamma = 120°$. Moreover, self-assembled monolayers of long-chain alcohols function as ice nucleators[35] and seem therefore capable of organizing water molecules at the interface via hydrogen bonds. Theoretical studies examining the interfaces between hexanol monolayers and water predict that an average of two water molecules form hydrogen bonds with each hexanol molecule.[36] They also indicate that the terminal C–OH bond of the $C_\gamma C_\beta C_\alpha OH$ moiety can be in a trans or gauche conformation about the C_α–C_β bond with equal probability. This result shows that there remain uncertainties on the exact conformation of the alcohol molecules close to the interface. In particular, the lone pair of the oxygen atoms that makes possible hydrogen bonding with water molecules is all the more accessible when the C_α–OH bond sits perpendicular to the water surface. Work to get a more definite picture of the OH arrangement at the interface, based on the Bragg rod analysis and energy calculations using molecular models, is underway.[37]

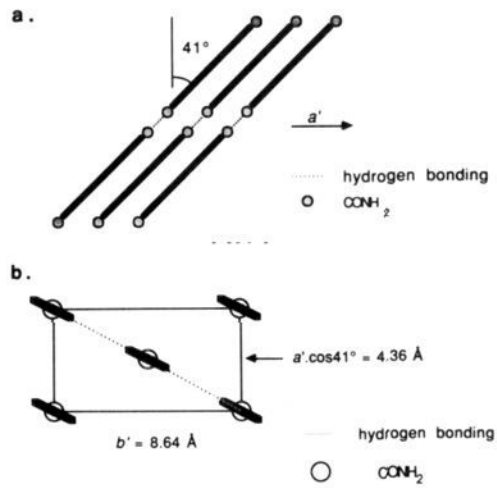

Figure 6. Schematic representation of the azelamide packing:[41] (a) view down b' of a single row in the bilayer, the mean axes of the hydrocarbon chains are symbolized by straight lines; (b) view down the molecular axis showing the centered rectangular cell, obtained by projection of the structure onto a plane perpendicular to the molecular axis; the black sticks symbolize the cross section of the carbon chain projected onto this plane.

Structure of the Acid Crystallites. In the carboxylic acid crystallites, the molecular tilt is in the direction of the short a axis of the rectangular unit cell, as in the layers of the β form of long-chain acid crystals.[16] The β_2 modification is relevant since the molecular tilt from the normal relative to the layer plane is about 26°. An example of such a crystal structure is the B form of stearic acid.[38] The tilt of 26° yields, in the layer of the 3-D crystal, unit cell parameters $a' = a'_s/\cos 26° = 5.54$ Å and $b' = b'_s = 7.42$ Å, compared with $a = 5.53$ Å and $b = 7.44$ Å in the 2-D crystallites. This match indicates that the chain packing in both systems is very similar. We therefore propose that in the acid crystallites the rectangular unit cell is primitive,[32] the chains are related by glide symmetry in the 2-D space group[33] *pg*, the glide being parallel to the a axis as shown in Figure 4b, and the packing is of the orthorhombic $O_\perp$ type. It is noteworthy that in spite of the dramatic difference in the environment of the polar head group in the 3-D crystal (in which the carboxylic groups form hydrogen-bonded cyclic dimers) and at the interface of a 2-D crystal bound to water, the hydrocarbon chains still pack in a similar manner. Note that in the 3-D crystal of B stearic acid,[38] the conformation about the C_α–C_β bond of the $HO_2CC_\alpha C_\beta C$ system is *cis*. We are currently investigating the possible head group arrangements at the monolayer–water interface, a more detailed analysis of the Bragg rod data will certainly provide more definite results concerning the exact molecular packing.[39]

The monolayer structures of shorter chain acids ($n = 19, 21$) studied under similar temperature and surface pressure conditions have been reported[9] (the corresponding phase was labeled L_2 in ref 9c). The results were very similar. The chains tilt toward nearest neighbors; for behenic acid[9c] ($n = 19$) the reported molecular tilt with respect to the surface normal is $t = 29°$ at zero pressure, and varies continuously under compression.

Structure of the Amide Crystallites. We could not find 3-D crystal structures of long-chain primary amides with a chain packing similar to the chain packing in the amide 2-D crystallites.[40] Long-chain diamide crystal structures proved more adequate to glean information on the chain packing in the 2-D crystallites.[41] It appears that in 3-D crystals of amides and diamides the van der Waals interactions between the chains are controlled by a

(31) (a) Nevertheless, a tilt of about 10° of the alcohol molecules in the direction of the b'_s axis would yield a layer structure that was calculated as one of the stable layer structures for long aliphatic alcohols, namely the γ_1 modification.[31b] For this modification, $a' = 4.98$ Å, $b' = 7.42/\cos 10° = 7.53$ Å, compared with average values of $a = 5.00$ Å and $b = 7.53$ Å measured in the alcohol 2-D crystallites. (b) Precht, D. *Kiel. Milchwirtsch. Forschungsber* **1974**, *26*, 221.

(32) Note that in the early sections of this paper, we have described the rectangular cells as centered. The term "centered" is not rigorously correct since a centered cell contains two molecules related by translation at X,Y and $^1/_2 + X, ^1/_2 + Y$. In the alcohol and acid crystallites, the molecules are not related by translation but by a glide, so that the cell contains a molecule at X,Y and one at $^1/_2 + X, ^1/_2 - Y$ or $^1/_2 - X, ^1/_2 + Y$ if the glide plane lies parallel to the a axis at $Y = ^1/_4$ or to the b axis at $X = ^1/_4$, respectively.

(33) (a) Possible molecular packing arrangements in a primitive rectangular cell limit the 2-D space groups[33b,c] to *pg*, *pmg*, *cm*, *p2gg*, *c2mm*. The *c2mm* space group is ruled out since the centered rectangular cell would contain two molecules each at the intersection of two mirror planes. The space groups *pmg* and *cm* would preclude the orthorhombic $O_\perp$ motif for the acid and alcohols monolayers and would involve too short a hydrogen-bonding axis in the amide monolayer since the hydrocarbon chains would lie on a mirror plane. These three space groups are therefore highly improbable. In the specific case of the alcohols, the Bragg rod diffraction data are sensitive enough to rule them out completely.[37] Finally, the possible molecular arrangements in the *p2gg* space group were examined; none of them could account for the observed in-plane diffraction data. This leaves us with space group *pg* in a primitive unit cell for the alcohol and the acid crystallites. For the amide crystallites, only an arrangement with space group *p*1 in a centered unit cell is consistent with the diffraction data and yields reasonable hydrogen-bonding distances. A detailed report of these arguments will be found in future publications on the alcohols,[37] the carboxylic acids,[39] and the primary amide.[42] (b) *International Tables for X-ray Crystallography*; Kynoch Press: Birmingham, **1965**; Vol. 1, pp 57–72. (c) Gavezotti, A.; Simonetta, M. *Comp. Maths with Appls.* **1986**, *12B*, 465.

(34) (a) Megaw, H. D. *Nature* **1934**, *134*, 900. (b) Owston, P. G.; Lonsdale, K. *J. Glaciol.* **1948**, *1*, 118.

(35) Gavish, M.; Popovitz-Biro, R.; Lahav, M.; Leiserowitz, L. *Science* **1990**, *250*, 973.

(36) Gao, J.; Jorgensen, W. L. *J. Phys. Chem.* **1988**, *92*, 5813.

(37) Wang, J. L. et al. Work in progress.

(38) (a) von Sydow, E. *Acta Crystallogr.* **1955**, *8*, 557. (b) Goto, M.; Asada, E. *Bull. Chem. Soc. Jpn.* **1978**, *51*, 2456.

(39) Leveiller, F. et al. Work in progress.

(40) (a) Leiserowitz, L.; Hagler, A. T. *Proc. R. Soc. London* **1983**, *A388*, 133. (b) Turner, J. D.; Lingafelter, E. C. *Acta Crystallogr.* **1955**, *8*, 551.

(41) Hospital, M. *Acta Crystallogr.* **1971**, *B27*, 484.

network of hydrogen bonds at the amide groups, so that in spite of relatively long hydrocarbon chains, the lateral chain interactions are insufficient to favor one of the common modes of hydrocarbon chain packing.[16,25] The unit cell parameters deduced from the GID data (Table I) suggest that this feature also applies to the 2-D crystallite structure of the amide monolayer. To develop further the argument, we consider the packing in the 3-D crystal of the diamide azelamide.[41] The molecules crystallize in bilayers characterized by unit cell axes $a' = 5.78$, $b' = 8.64$ Å. Within the bilayer, the molecules form linear dimers. These chain dimers are stacked by translation along the a' axis (Figure 6a). The molecular chains are tilted by 41° vis-à-vis the normal to the $a'b'$ plane. The projection of a single layer of molecules down the mean molecular axis is shown in Figure 6b. In the layer, the molecules are related by translation to form a close-packed array characterized by a projected cell $a'(\cos 41°) = 4.36$ Å, $b' = 8.64$ Å which is centered. These molecules are interlinked by N-H···O hydrogen bonds via translation symmetry, the hydrogen bonds being parallel to the diagonal of the projected unit cell of length 9.68 Å (Figure 6b). We propose a similar motif in the monolayer crystallites: the chains are stacked into rows by translation along the 4.69-Å axis with the molecular axis tilted at an angle of 18° to the normal of the ab plane, which is parallel to the water surface. The molecules form a close-packed array characterized by a projected cell $a(\cos 18°) = 4.46$ Å, $b = 8.69$ Å which is centered. These molecules are interlinked by N-H···O hydrogen bonds via translation symmetry, the hydrogen bonds being parallel to the diagonal of the projected unit cell of length 9.77 Å. Thus, the 2-D space group[33] is, this time, $p1$.

Crystallite Correlation Lengths. Let us now consider the X-ray reflection widths and the resulting extent of crystalline lateral ordering; in other words, the positional correlation length[19] data. For all the measured monolayer crystals, there are large differences in the width of the two first-order reflections (Table I), which indicates an anisotropy of the extent of crystalline lateral ordering. The positional correlation length L of the crystallites is smaller along the direction of the molecular tilt. Indeed, for the alcohol (X = OH) monolayers, L is in the range of 60–95 spacings along the molecular tilt axis b, but along the perpendicular axis a, L extends over at least 240 spacings. For the acid (X = COOH) and the amide ($X = CONH_2$) monolayers, L covers only 35 and 45 spacings, respectively, along the a axis,[43] the direction of molecular tilt; along the perpendicular axis b, L extends over at least 270 spacings for the acid and 135 spacings for the amide. These results suggest that these monolayer crystals are strips elongated perpendicular to the molecular tilt direction. The same observation was made in the L_2 phase of behenic acid.[9c] It would be interesting to understand the relationship between the amphiphile structure and the monolayer crystal morphology. Such a study requires a more detailed knowledge of the intermolecular interactions involved in the stabilization of the crystal.

Conclusion

This report provides evidence that the self-organization into 2-D crystallites of insoluble amphiphilic molecules at the air–water interface is a widespread phenomenon. The evidence is very strong that for the aliphatic amphiphilic alcohol and acid molecules studied here the 2-D space group is pg; thus, the rectangular cell is primitive, not centered. The 2-D space group for the aliphatic amphiphilic amide molecules is $p1$, thus in this case the rectangular cell is centered. The study also reveals the similarity of molecular packing arrangements in the 2-D crystals floating on water to those in their 3-D counterparts. This point is relevant to the observation that head-group arrangements of 2-D crystalline assemblies similar to layer arrangements of given 3-D crystals were found to function as nucleators for these 3-D crystals. Numerous examples have been reported in this expanding field: ice nucleation under alcohol monolayers[35] for which there appears to be a lattice match between the alcohol crystallites and the attached face of hexagonal ice, inorganic crystals underneath stearic acid monolayers,[44] glycine,[3] and p-hydroxybenzoic acid[45] under monolayers whose head groups are recognized by the solute molecules. Also, since growing 2-D crystals are dynamic entities, constantly interacting with the solvent or additives in solution, a full understanding of the mechanisms of their nucleation and growth would shed light on the corresponding mechanisms involved in 3-D crystal growth. Surface diffraction techniques will provide a direct means of exploration of these mechanisms at the molecular level. A future expansion of such studies will involve organized assemblies of amphiphiles at liquid–liquid interfaces. Such interfaces would provide a closer simulation of crystallization processes in solution, since the hydrophobic chains of the molecules would also interact with a solvent. These systems, for the same reason, would be more suitable models for studying membrane biology.

Acknowledgment. We thank Ada Yonath of the Max Planck Unit for Structural Molecular Biology for use of laboratory facilities, Edna Shavit for the synthesis of the alcohol compounds, and Christine Böhm for help during the measurements at the synchrotron beam line. We acknowledge financial support from the German Israeli Foundation (GIF), the donors of the Petroleum Research Fund, administered by the American Chemical Society, and the Danish Foundation for Natural Sciences and HASYLAB, DESY, Hamburg, FRG for beam time.

Registry No. $C_{29}H_{59}COOH$, 506-50-3; $C_{30}H_{61}OH$, 593-50-0; $C_{23}H_{47}OH$, 3133-01-5; $C_{31}H_{63}OH$, 544-86-5; $C_{19}H_{39}CONH_2$, 51360-63-5.

(42) Weinbach, S. P. et al. Work in progress.

(43) Although the positional correlation length L was not determined along the a axis for the acid and amide systems, but rather along the reciprocal directions $\mathbf{a}^* \pm \mathbf{b}^*$, it stands to reason that along the a axis L can hardly be larger than along $(\mathbf{a}^* \pm \mathbf{b}^*)$.

(44) (a) Landau, E. M.; Popovitz-Biro, R.; Levanon, M.; Leiserowitz, L.; Lahav, M. *Mol. Cryst. Liq. Cryst.* **1986**, *134*, 323. (b) Mann, S.; Heywood, B. R.; Rajam, S.; Birchall, J. D. *Nature* **1988**, *334*, 692.

(45) Weissbuch, I.; Berkovic, G.; Lahav, M.; Leiserowitz, L. *J. Am. Chem. Soc.* **1990**, *112*, 5874.